

RADIATIVE CORRECTIONS IN THE MSSM HIGGS SECTOR

WOLFGANG HOLLIK

*Institut für Theoretische Physik, Universität Karlsruhe
D-76128 Karlsruhe, Germany*

E-mail: hollik@itpaxp3.physik.uni-karlsruhe.de

ABSTRACT

1-loop diagrammatic calculations of cross sections and decay widths of neutral Higgs bosons in the minimal supersymmetric standard model are reviewed and compared with compact expressions in the effective potential approximation.

1. Introduction

In order to experimentally detect possible signals from the Higgs sector of the minimal supersymmetric standard model (MSSM), detailed studies for the decay and production processes of Higgs bosons are required. As discovered several years ago ^{1,2,3}, radiative corrections in the MSSM Higgs sector are large and have to be taken into account for phenomenological studies. Three main approaches have been developed to calculate the 1-loop radiative corrections to the MSSM Higgs boson masses, production and decay rates:

- (i) The Effective Potential Approach (EPA) ².
- (ii) The method of Renormalization Group Equations (RGE) ³.
- (iii) The diagrammatic calculation in the on-shell renormalization scheme (Feynman Diagram Calculation, FDC) ^{4,5,6,7,8,9}: The masses are calculated from the pole positions of the Higgs propagators, and the cross sections are obtained from the full set of 1-loop diagrams contributing to the amplitudes.

The method (iii) is technically involved, but it is the most accurate one at the 1-loop level and can be used as a reference frame for simpler approximations. The searches for Higgs bosons at LEP ¹⁰ and studies for the future searches at higher energies ¹¹ conventionally make use of the very compact formulation in the effective potential approximation.

This talk gives an overview on the neutral MSSM Higgs sector at the 1-loop level. The results for the cross sections of neutral Higgs production processes in e^+e^- collisions and for the neutral Higgs decay widths are discussed in a complete diagrammatic calculation and compared, where possible, with the corresponding ones of the compact EPA approximation.

2. One-loop calculations

The tree level potential for the neutral MSSM Higgs bosons can be written as follows:

$$V = m_1^2 H_1^2 + m_2^2 H_2^2 + \epsilon_{ij}(m_{12}^2 H_1^i H_2^j + H.c.) + \frac{g^2 + g'^2}{8}(H_1^2 - H_2^2)^2 + \frac{g^2}{4}(H_1 H_2)^2. \quad (1)$$

Diagonalization of the mass matrices for the CP-even and the CP-odd scalars, following from the potential (1), leads to three physical particles: two CP-even Higgs bosons H^0, h^0 and one CP-odd Higgs boson A^0 , and defines their tree-level masses m_h, m_H, m_A and the mixing angles α, β . For a systematic 1-loop calculation, the free parameters of the Higgs potential $m_1^2, m_2^2, m_{12}^2, g, g'$ and the two vacua v_1, v_2 are replaced by renormalized parameters plus counter terms. This transforms the potential V into $V + \delta V$, where V , expressed in the renormalized parameters, is formally identical to (1), and δV is the counter term potential. The counter terms are fixed by seven renormalization conditions. In the on-shell scheme they can be chosen as follows:

- the on-shell conditions for $M_{W,Z}$ and the electric charge e as in the minimal standard model.
- the on-shell condition for the A^0 boson with the pole mass M_A .
- the tadpole conditions for vanishing renormalized tadpoles:

$$T_H + \delta t_H = 0, \quad T_h + \delta t_h = 0$$

where $T_{H,h}$ are the sum of the 1-loop tadpole diagrams for H^0 and h^0 , and $\delta t_{H,h}$ are the tadpole counter terms following from (1). These conditions ensure that v_1, v_2 are the minima of the potential at the 1-loop level.

- the renormalization of $\tan \beta$ in such a way that the relation $\tan \beta = v_2/v_1$ is valid for the 1-loop Higgs minima.

By this set of conditions, the input for the MSSM Higgs sector is fixed by M_A and $\tan \beta$, together with the standard gauge sector input $M_{W,Z}$ and e . The last condition on $\tan \beta$ can only be imposed in connection with an appropriate field renormalization of the two Higgs doublet fields. Together with the gauge field renormalization one has four extra renormalization constants which can be fixed as in the standard model gauge sector¹², extended by two more conditions for the Higgs sector. The latter two have been treated in two slightly different ways^{5,6} in the literature; physical results,

however, differ only marginally by unobservably small terms. The corresponding 1-loop physical Higgs boson masses M_h^2, M_H^2 are obtained as the pole positions of the dressed scalar propagators.

In the EPA, the tree level potential is improved by adding the 1-loop terms. The 1-loop potential $V^{(1)}$ is re-diagonalized yielding the 1-loop corrected physical masses M_H, M_h and the effective mixing angle α_{eff} . These improved masses and α_{eff} are used in the Born formulae for production and decay rates of Higgs bosons. In the approximation keeping only the dominating terms $\sim m_t^4$, the expressions read ²:

$$M_{H,h}^2 = \frac{M_A^2 + M_Z^2 + \epsilon_t + \sigma_t}{2} \pm \left[\frac{(M_A^2 + M_Z^2)^2 + (\epsilon_t - \sigma_t)^2}{4} - M_A^2 M_Z^2 \cos^2 2\beta + \frac{(\epsilon_t - \sigma_t) \cos 2\beta}{2} (M_A^2 - M_Z^2) - \lambda_t \sin 2\beta (M_A^2 + M_Z^2) + \lambda_t^2 \right]^{1/2} \quad (2)$$

with

$$\begin{aligned} \epsilon_t &= \frac{N_C G_F m_t^4}{\sqrt{2} \pi^2 \sin^2 \beta} \left[\log \left(\frac{m_{\tilde{t}_1} m_{\tilde{t}_2}}{m_t^2} \right) + \frac{A_t (A_t + \mu \cot \beta)}{m_{\tilde{t}_1}^2 - m_{\tilde{t}_2}^2} \log \frac{m_{\tilde{t}_1}^2}{m_{\tilde{t}_2}^2} \right. \\ &\quad \left. + \frac{A_t^2 (A_t + \mu \cot \beta)^2}{(m_{\tilde{t}_1}^2 - m_{\tilde{t}_2}^2)^2} \left(1 - \frac{m_{\tilde{t}_1}^2 + m_{\tilde{t}_2}^2}{m_{\tilde{t}_1}^2 - m_{\tilde{t}_2}^2} \log \frac{m_{\tilde{t}_1}}{m_{\tilde{t}_2}} \right) \right] \\ \lambda_t &= \frac{N_C G_F m_t^4}{\sqrt{2} \pi^2 \sin^2 \beta} \left[\frac{\mu (A_t + \mu \cot \beta)}{m_{\tilde{t}_1}^2 - m_{\tilde{t}_2}^2} \log \frac{m_{\tilde{t}_1}^2}{m_{\tilde{t}_2}^2} \right. \\ &\quad \left. + \frac{2\mu A_t (A_t + \mu \cot \beta)^2}{(m_{\tilde{t}_1}^2 - m_{\tilde{t}_2}^2)^2} \left(1 - \frac{m_{\tilde{t}_1}^2 + m_{\tilde{t}_2}^2}{m_{\tilde{t}_1}^2 - m_{\tilde{t}_2}^2} \log \frac{m_{\tilde{t}_1}}{m_{\tilde{t}_2}} \right) \right] \\ \sigma_t &= \frac{N_C G_F m_t^4}{\sqrt{2} \pi^2 \sin^2 \beta} \frac{\mu^2 (A_t + \mu \cot \beta)^2}{(m_{\tilde{t}_1}^2 - m_{\tilde{t}_2}^2)^2} \left[1 - \frac{m_{\tilde{t}_1}^2 + m_{\tilde{t}_2}^2}{m_{\tilde{t}_1}^2 - m_{\tilde{t}_2}^2} \log \frac{m_{\tilde{t}_1}}{m_{\tilde{t}_2}} \right]. \quad (3) \end{aligned}$$

The approximate effective mixing angle α_{eff} is determined by

$$\tan \alpha_{eff} = \frac{-(M_A^2 + M_Z^2) \sin \beta \cos \beta + \lambda_t}{M_Z^2 \cos^2 \beta + M_A^2 \sin^2 \beta + \sigma_t - M_h^2}. \quad (4)$$

These formulae contain the masses $m_{\tilde{t}_{1,2}}$ of the top squarks, the Higgs mixing parameter μ of the superpotential, and the non-diagonal entry A_t in the stop mass matrix. This matrix is diagonal for $A_t + \mu \cot \beta = 0$. In this special case we have $\sigma_t = \lambda_t = 0$, and only the ϵ_t term contributes.

Recently the leading 2-loop corrections to the CP-even MSSM Higgs boson masses have been investigated, based on the EPA and RGE methods ¹³. The main conclusion

is that 2-loop corrections are also significant and tend to compensate partially the effects of the 1-loop corrections.

3. Production cross sections for $e^+e^- \rightarrow Zh^0(H^0), A^0h^0(H^0)$

In this section the results for $Z^0H^0(Z^0h^0)$ and $A^0H^0(A^0h^0)$ production are shown as derived from the complete 1-loop FDC, and the quality of the corresponding EPA results is discussed. The formulae for the cross sections obtained in the FDC differ from the Born expressions not only by the corrections to the masses and to the angle α , but also by new form factors and momentum dependent effects (see ^{5,8} for analytic expressions).

For the calculations of the cross sections we need the full set of 2-, 3- and 4-point functions. In Fig. 1 the diagrams contributing to $e^+e^- \rightarrow Z^0h^0(H^0)$ are collected. The diagrams for $e^+e^- \rightarrow A^0h^0(H^0)$ can be obtained by changing Z^0 into A^0 on the external line and skipping the diagrams i), j).

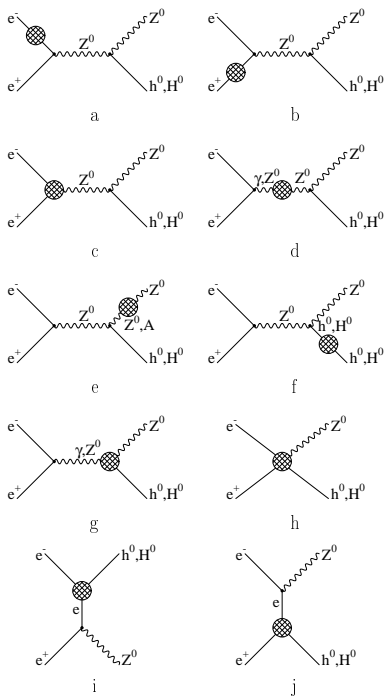


Figure 1: Classes of diagrams contributing to the $e^+e^- \rightarrow Z^0h^0(H^0)$ process in the FDC approach.

In the figures of this section the set of parameters (in GeV): $M_A = 200$, $M_2 = 1000$, $\mu = 500$, $M_{sl} = 300$, $M_{sq} = 1000$, $A_t = A_b = 1000$ is used as an example. μ is the parameter describing the Higgs doublet mixing in the MSSM superpotential. M_2 denotes the SU(2) gaugino mass parameter. For the U(1) gaugino mass we use the

value $M_1 = \frac{5}{3} \tan^2 \theta_W M_2$, suggested by GUT constraints. M_{sq} , M_{sl} , A_t and A_b are the parameters entering the sfermion mass matrices. For simplicity we assume a common value M_{sq} for all generations of squarks, and a common M_{sl} for sleptons.

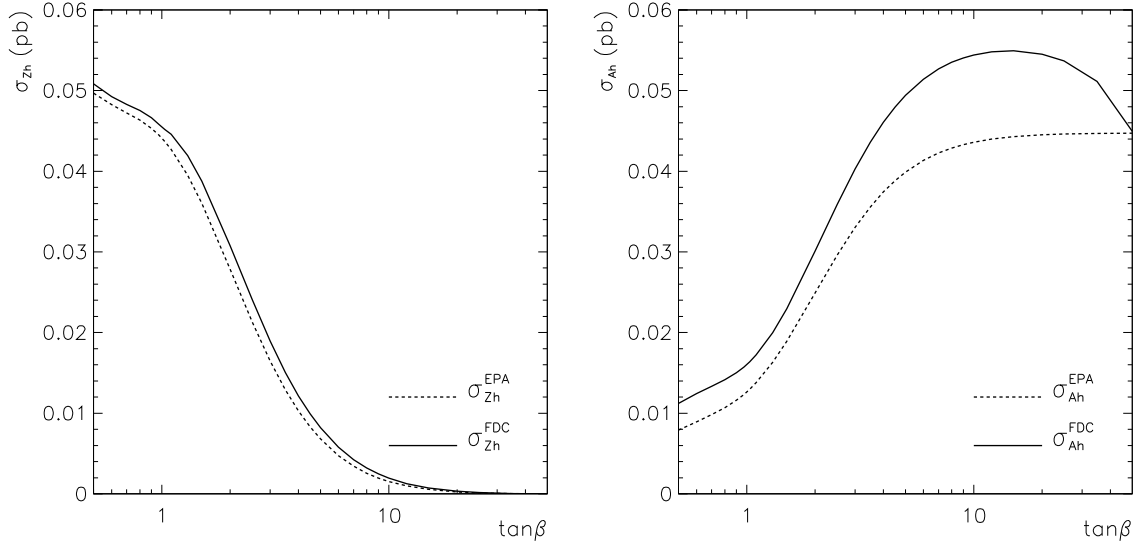


Figure 2: Comparison of the cross sections $\sigma(e^+e^- \rightarrow Z^0 h^0, A^0 h^0)$ obtained in the EPA and FDC. $\sqrt{s} = 500$ GeV.

In the conventional $M_A, \tan \beta$ parametrization, Fig. 2 shows the production cross sections $\sigma(e^+e^- \rightarrow Z^0 h^0, A^0 h^0)$ at $\sqrt{s} = 500$ GeV. For the chosen set of parameters the numerical differences can reach 30% at $\sqrt{s} = 500$ GeV. Note, however, that in the region of large cross sections the EPA accuracy is better (20% at 500 GeV). The situation of H^0 production is very similar. The differences between EPA and FDC become more important with increasing energies, exceeding 40% at 1 TeV. Also the effect of the additional form factors in the FDC grows, which modify the angular dependence of the cross section compared to the effective Born approximation. More detailed discussions can be found in ref. ^{9,11}.

A more physical parametrization of the cross sections is given in terms of the two Higgs boson masses M_A and M_h (or M_H), instead of the formal quantity $\tan \beta$. This parametrization is more involved in the calculations, but it has the advantage of physically well defined input quantities avoiding possible confusions from different renormalization schemes. Varying e.g. M_H (M_A and other input quantities fixed) we obtain $\tan \beta$ and σ_{ZH}, σ_{AH} as functions of M_H . Significant differences can occur for the cross sections, as displayed in Fig. 3 where the predictions of EPA and FDC for the σ_{ZH} and σ_{AH} are plotted as functions of M_H . The typical size of the differences between the methods is 10-20% for $\sqrt{s} = 500$ GeV, but they may become quite large (60%) for the process $\sigma(e^+e^- \rightarrow Z^0 H^0)$. In other cases, they are of the order 10-20%.

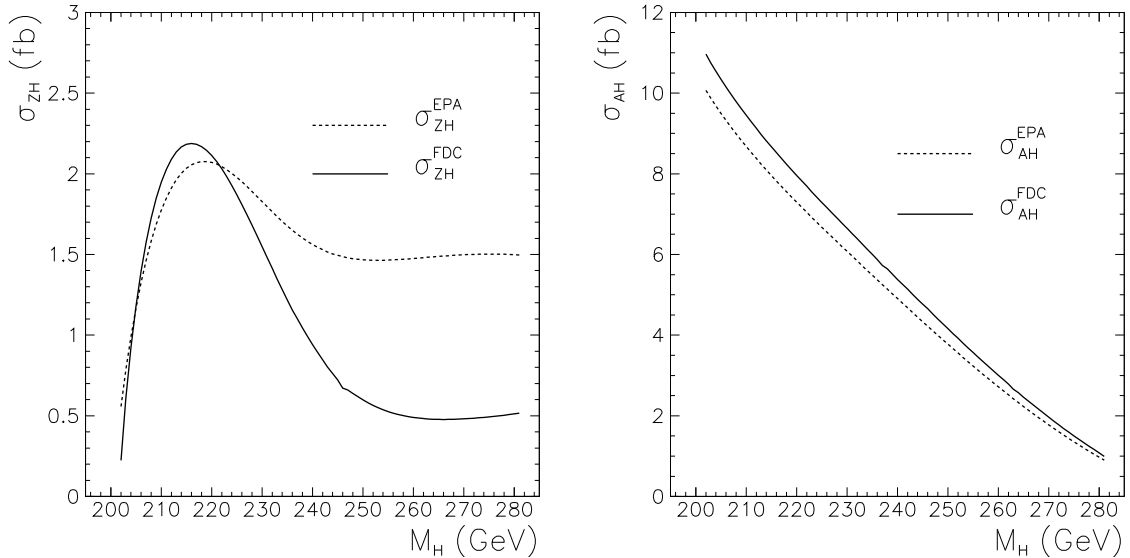


Figure 3: Comparison of the cross sections $\sigma(e^+e^- \rightarrow Z^0 H^0, A^0 H^0)$ versus M_H in the EPA and FDC. $\sqrt{s} = 500$ GeV.

The variation of the SUSY parameters: sfermion and gaugino masses, μ parameter and sfermion mixing parameters, does not have a large effect on the size of the differences between the EPA and FDC. Hence, the figures represent typical examples.

Summarizing this section, comparisons between the FDC and EPA predictions have shown that at $\sqrt{s} = 500$ GeV the EPA has an accuracy of typically 10-20% in the parameter regions where the cross sections are large. The differences become larger with increasing energy, where also modifications of the Born-like angular distributions are more visible. The use of the physical input variables M_A , M_h or M_A , M_H avoids ambiguities from the definition of $\tan\beta$ in higher order, but the observed differences remain of the same size. For a better accuracy, the full FDC would be required.

So far the leading 2-loop terms have not been incorporated. They would improve the 1-loop FDC results in the same way as the approximations and thus do not influence the remaining differences which can only be obtained by an explicit diagrammatic calculation.

Loop-induced pair production $e^+e^- \rightarrow h^0 h^0, H^0 H^0, h^0 H^0, A^0 A^0$ of neutral Higgs bosons have also been studied recently¹⁴, as well as associated Higgs-photon production $e^+e^- \rightarrow \gamma h^0 (H^0, A^0)$ ¹⁵. The general result is that the cross sections in the MSSM are not enhanced by the extra non-standard particles in the loops, $\sigma(MSSM) \leq \sigma(SM)$. In the decoupling limit, for heavy SUSY particles, the standard model results are recovered. For detailed studies of the virtual SUSY effects in the loop-induced Higgs- γZ and Higgs- $\gamma\gamma$ couplings see ref.¹⁶.

4. Decays of neutral Higgs bosons

The decay widths (the branching ratios, respectively) as well as the mass–width correlations are quantities which can help to differentiate between Higgs bosons of different origin. Except for a small region of the parameter space, the light neutral Higgs of the MSSM decays predominantly into b -quarks and τ -leptons; the heavier ones H^0 and A^0 can have significant decay modes also into top quarks, scalar quarks, and neutralinos/charginos. In a certain region of the parameter space, also the decay $h^0 \rightarrow A^0 A^0$ is allowed. Loop-mediated decay processes are the hadronic decay modes into gluons¹⁷ and gluinos¹⁸.

4.1. Fermionic decays

For the important fermionic decays both electroweak and QCD corrections^{7,19,20} have been calculated. The standard QCD corrections¹⁹ for $\phi \rightarrow q\bar{q}$, $\phi = h^0, H^0, A^0$, are large. The bulk can be absorbed into the running quark mass by replacing the pole mass according to $m_q \rightarrow \bar{m}_q(M_\phi)$. The SUSY-QCD corrections arising from virtual gluinos and squarks^{7,20} can also become remarkably large, in particular for large values of μ and $\tan\beta$ where they can reach up to 30%.

The set of 1-loop electroweak corrections to $h^0 \rightarrow f\bar{f}$ can be summarized in terms the following decay amplitude:

$$A(h \rightarrow f\bar{f}) = \sqrt{Z_h} \left(\Gamma_h - \frac{\Sigma_{hH}(M_h^2)}{M_h^2 - m_H^2 + \Sigma_{HH}(M_h^2)} \Gamma_H \right) \quad (5)$$

with the renormalized self-energies Σ and 3-point vertex functions $\Gamma_{h,H}$. The amplitude for $H^0 \rightarrow f\bar{f}$ is obtained by interchanging $h \leftrightarrow H$. The wave function renormalization $Z_{h(H)}$ is the finite residue of the h^0 (H^0) propagator. The amplitude for $A^0 \rightarrow f\bar{f}$ is given by the renormalized vertex Γ_A alone, due to the renormalization condition $Z_A = 1$ ⁶. For the absolute decay widths, in order to have the correct normalization in terms of the Fermi constant G_F , the MSSM correction to the muon lifetime, i.e. the quantity Δr , has to be taken into account²¹. It drops out in the branching ratios. The inclusion of the mixing term in eq. (5) corresponds essentially to the re-diagonalization of the mass matrix in the EPA. In the EPA, one obtains the improved decay amplitude by using the EPA masses and the effective mixing angle α_{eff} , eq. (4), in the Born expression for the vertex Γ_h , with $Z_h = 1$ and $\Sigma_{hH} = 0$ in eq. (5). As shown in⁷, the EPA is a very good approximation of the full 1-loop result for the fermionic branching ratios, with exception of extremely low values for $\tan\beta$ (see Fig. 4).

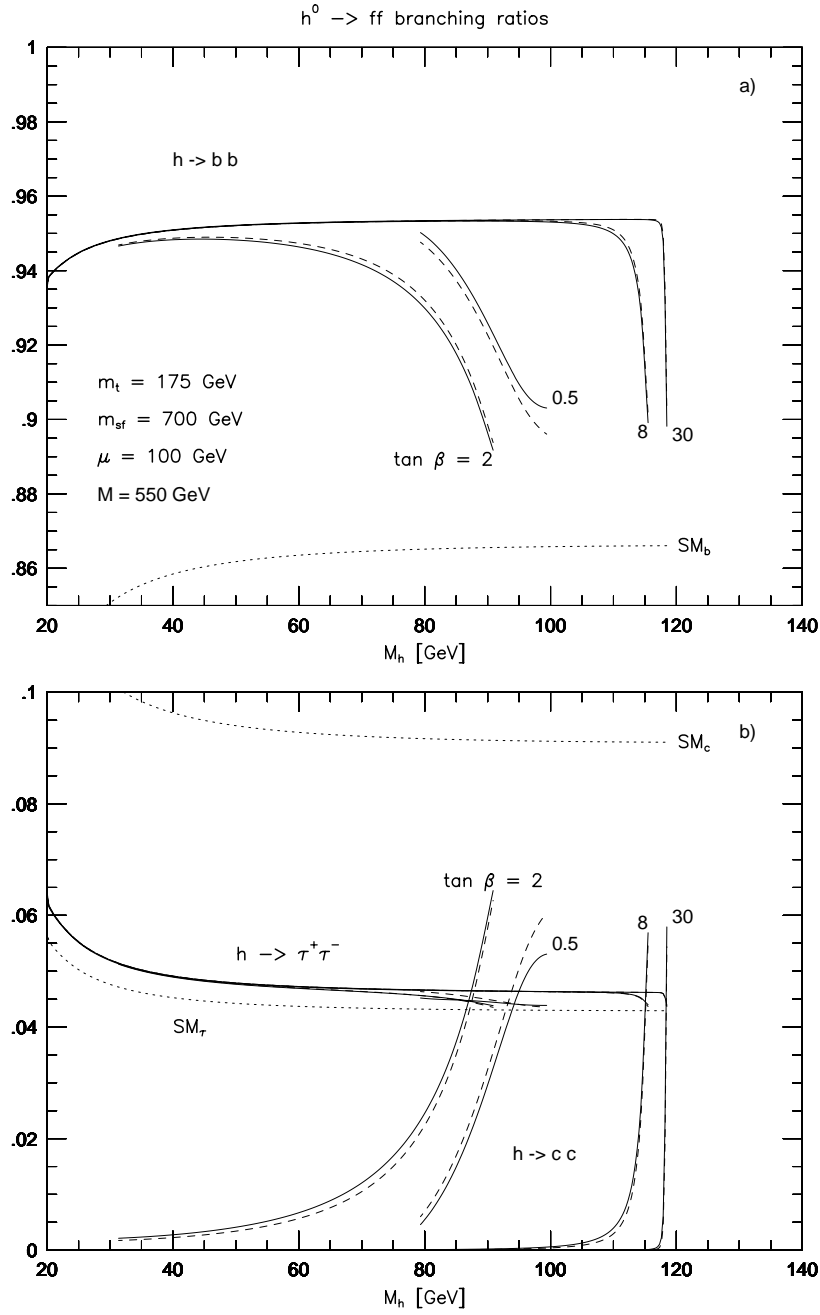


Figure 4: Fermionic branching ratios Higgs decays into fermion pairs (from ⁷). EPA: dashed lines; complete 1-loop: full lines. M denotes the SU(2) gaugino mass.

4.2. The decay $h^0 \rightarrow A^0 A^0$

A specific consequence of the large radiative corrections to the h^0 mass is the possibility of having $M_h > 2M_A$, which makes the decay $h^0 \rightarrow A^0 A^0$ kinematically allowed at 1-loop order for low values of $\tan\beta$ and M_A . In the allowed region it turns out to be the dominant decay mode, with branching ratios of 0.8–0.9. The decay width was obtained in the EPA (last reference of ²), by use of the RGE ²², and by a complete diagrammatic 1-loop calculation ²³. A simple approximate formula for the decay amplitude, which reproduces the full 1-loop decay width at an accuracy within typically 10%, is given by ²³

$$A(h^0 \rightarrow A^0 A^0) = -\frac{g}{2c_W} M_Z \cos 2\beta \sin(\alpha_{eff} + \beta) + \Delta V \quad (6)$$

with α_{eff} from (4) and

$$\Delta V \simeq \frac{3g^3}{16\pi^2 M_W^3} \frac{\cos \alpha_{eff}}{\sin \beta} \cot^2 \beta \left[m_t^4 \log \frac{m_t^2}{m_{\tilde{t}_1} m_{\tilde{t}_2}} - (A_t - \mu \tan \beta)^2 m_t^4 \frac{\log m_{\tilde{t}_1} - \log m_{\tilde{t}_2}}{m_{\tilde{t}_1}^2 - m_{\tilde{t}_2}^2} + m_t^2 \frac{M_h^2 - 2M_A^2}{2} \right] \quad (7)$$

which arises from the vertex correction diagrams with virtual top and stop quarks. It contributes significantly to the decay amplitude in particular for $\tan\beta \simeq 1$, where the improved Born approximation [the first term in eq. (6)] is very small. The second term in ΔV is also sizeable for intermediate masses of the top squarks. For details see ref. ²³.

4.3. Higgs decays into squark pairs

In a large part of the MSSM parameter space, the decays into squark pairs $H^0, A^0 \rightarrow \tilde{q}\tilde{q}$ can be the dominant decay modes ²⁴. QCD corrections from gluons and gluinos have been calculated recently ²⁵. They are sizeable (up to 50%) and should be taken into account for phenomenological studies.

References

1. S. P. Li, M. Sher, *Phys. Lett.* **B140** (1984), 339; J. Gunion, A. Turski, *Phys. Rev.* **D39** (1989) 2701; **D40** (1989) 2325, 2333; M. Berger, *Phys. Rev.* **D41** (1990) 225.
2. J. Ellis, G. Ridolfi, F. Zwirner, *Phys. Lett.* **262B** (1991) 477; R. Barbieri, M. Frigeni, *Phys. Lett.* **258B** (1991) 395; A. Brignole, J. Ellis, G. Ridolfi, F. Zwirner *Phys. Lett.* **271B** (1991) 123.

3. H.E. Haber, R. Hempfling, *Phys. Rev. Lett.* **66** (1991) 1815; *Phys. Rev.* **D48** (1993) 4280; M. Carena, K. Sasaki, C.E.M. Wagner, *Nucl. Phys.* **381B** (1992) 66. P.H. Chankowski, S. Pokorski, J. Rosiek, *Phys. Lett.* **281B** (1992) 100.
4. A. Brignole, *Phys. Lett.* **281B** (1992) 284.
5. P. Chankowski, S. Pokorski, J. Rosiek *Nucl. Phys.* **B423** (1994) 437; **B423** (1994) 497.
6. A. Dabelstein, W. Hollik, in: e^+e^- Collisions at 500 GeV, DESY 92-123C, ed. P. Zerwas; A. Dabelstein, *Z. Phys.* **C67** (1995) 495.
7. A. Dabelstein, *Nucl. Phys.* **B456** (1995) 25.
8. V. Driesen, W. Hollik, *Z. Phys.* **C68** (1995) 485.
9. V. Driesen, W. Hollik, J. Rosiek, *Z. Phys.* **C71** (1996) 259.
10. P. Mättig, *28th International Conference on High Energies*, Warsaw 1996 (plenary talk); *Higgs Physics*, M. Carena, P. Zerwas et al., in: *Physics at LEP2*, CERN 96-01, CERN 1996, eds. G. Altarelli, T. Sjöstrand, F. Zwirner.
11. *Higgs Particles*, in: e^+e^- Collisions at 500 GeV, DESY 92-123A,B,C,D, ed. P. Zerwas.
12. M. Böhm, W. Hollik, H. Spiesberger, *Fortschr. Phys.* **34** (1986) 687; W. Hollik, *Fortschr. Phys.* **38** (1990) 165.
13. R. Hempfling, A. Hoang, *Phys. Lett.* **331B** (1994) 99; M. Carena, J.R. Espinosa, M. Quiros, C.E.M. Wagner, *Phys. Lett.* **355B** (1995) 209; M. Carena, M. Quiros, C.E.M. Wagner, *Nucl. Phys.* **B461** (1996) 407.
14. A. Djouadi, V. Driesen, C. Jünger, *Phys. Rev.* **D54** (1996) 759.
15. A. Djouadi, V. Driesen, W. Hollik, J. Rosiek, hep-ph/9609420, to appear in *Nucl. Phys. B*.
16. A. Djouadi, V. Driesen, W. Hollik, J.I. Illana, hep-ph/9612362; A. Djouadi, V. Driesen, W. Hollik, A. Kraft, hep-ph/9701342.
17. A. Djouadi, M. Spira, P. Zerwas, *Phys. Lett.* **264B** (1991) 440; M. Spira et al., *Nucl. Phys.* **B453** (1995) 17.
18. A. Djouadi, M. Drees, *Phys. Rev.* **D51** (1995) 4997.
19. E. Braaten, J.P. Leveille, *Phys. Rev.* **D22** (1980) 715; D. Bardin et al., *Yad. Fiz.* **53** (1991) 240; M. Drees, K. Hikasa, *Phys. Lett.* **276B** (1990) 455.
20. J.A. Coarasa, R.A. Jimenez, J. Solà, *Phys. Lett.* **389B** (1996) 312.
21. P. Chankowski et al., *Nucl. Phys.* **B417** (1994) 101; D. Garcia, J. Solà, *Mod. Phys. Lett.* **A9** (1994) 211.
22. H.E. Haber, R. Hempfling, Y. Nir, *Phys. Rev.* **D46** (1992) 3015.
23. S. Heinemeyer, W. Hollik, *Nucl. Phys.* **B474** (1996) 32.
24. A. Djouadi et al., hep-ph/9605339; A. Bartl et al., hep-ph/9607388.
25. A. Bartl et al., hep-ph/9701398; A. Arhrib, A. Djouadi, W. Hollik, C. Jünger, hep-ph/9702426.

